FROZEN NATURAL ORBITALS: SYSTEMATIC BASIS SET TRUNCATION FOR COUPLED-CLUSTER THEORY

Andrew G. TAUBE[1] and Rodney J. BARTLETT[2,*]
Department of Chemistry, University of Florida, Quantum Theory Project,
Gainesville, FL 32611, U.S.A.; e-mail: [1] taube@qtp.ufl.edu, [2] bartlett@qtp.ufl.edu

Received March 25, 2005
Accepted June 6, 2005

We are happy to contribute this paper to the Festschrift in honor of Joe Paldus' 70th birthday and wish him MANY HAPPY RETURNS!

The method of frozen natural orbital (FNO) basis set truncation for coupled-cluster theory is described. Numerical comparisons of the FNO potential energy surfaces of a group of small molecules at the CCSD(T) level in DZP, cc-pVTZ, cc-pVQZ bases show that truncation of up to 50% of the virtual space yields CC correlation energies that are accurate to 90 or 95% when added to the full MBPT(2) basis result. The FNO truncation method is also applied to dimethylnitramine (DMNA): both the equilibrium structure and dimer interactions, yielding results at the CCSD(T) level in both a DZP and cc-pVTZ basis set that agree with literature values. CCSD(T) calculations at two possible equilibrium structures of 1,3,5-trinitrohexahydro-1,3,5-triazine (RDX) in a truncated DZP basis are also reported.

Keywords: Coupled-cluster method; Natural orbital; Many-body perturbation theory; RDX; Reduced computational cost; FNO; *Ab initio* calculations; Quantum chemistry.

Dimethylnitramine (DMNA) is a model compound for combustion processes that occur in more complicated nitramines, such as 1,3,5-trinitrohexahydro-1,3,5-triazine (RDX) and 1,3,5,7-tetranitrooctahydro-1,3,5,7-tetrazocine (HMX). According to experimental data from both solid-phase X-ray crystallography[1] and gas-phase electron diffraction[2] measurements, the equilibrium geometry of DMNA should be planar – C_{2v}. However, single-molecule theoretical studies have consistently predicted a ground-state geometry with only C_s symmetry[3–6]. It has been suggested that these theoretical calculations may be more reliable than the experimental results[4–6]. Calculations have been performed using a variety of methods: restricted Hartree–Fock (RHF), many-body perturbation theory (MBPT(2)), multiple density functional methods (B3LYP, BLYP, PW91) and quadratic configuration interaction with singles and doubles (QCISD) in moderately sized

doi:10.1135/cccc20050837

bases, e.g. 6-31G*[7] or cc-pVDZ[8]. To have confidence in the theoretical predictions, especially with contradicting experimental data, it is often necessary to include at least through triple excitations (preferably within the coupled-cluster theory framework) and work in large basis sets.

When DMNA (or RDX or HMX) burns, it is not solely in the gas phase; ignition occurs in the crystalline solid phase[9]. Therefore, it is important to take into account the effect of intermolecular interaction on these molecules. The dimer of DMNA has been calculated at fixed monomer (C_{2v}) geometry with symmetry-adapted perturbation theory in a cc-pVDZ basis set[10]. This study identified five local minima for the interactions between the fixed monomers using a grid search across both angles and relative separations between the two monomers of DMNA, by including the effects of dispersion, exchange, induction and electrostatic interactions between monomers perturbatively.

In the solid phase, RDX has one of two forms: α-RDX, which has C_s symmetry, also called the axial–axial–axial (AAA) boat form, and β-RDX, which has C_{3v} symmetry, also called the AAA chair form, and is the experimental structure of the gas-phase RDX molecule. Results at MBPT(2) and various density functionals appear to agree, although all results are in moderate-to-small bases[11,12]. At least one study has questioned whether the α-RDX structure is a minimum of the lone molecule at all, suggesting instead a twisted non-symmetric conformation as the second gas-phase minimum[13].

To clarify the theoretical confusion, it would be valuable to apply predictive coupled-cluster theory, which requires at least perturbative triples (CCSD(T))[14–16] and a large basis set (triple zeta or better), to these molecules. The scaling of CCSD(T) with the number of unoccupied (virtual) Hartree–Fock orbitals is V^4, restricting the size of the molecules that can be computed. There are many attempts at circumventing this computational barrier, for example, localized orbitals[17,18], Cholesky decomposition[19], and the singular value decomposition approach[20,21]. Finally, $R12$ coupled-cluster theory[22–24] could provide nearly basis set limit results. Each of these methods is either complicated (requiring significant modification to standard programs), requires user input to identify regions that should be correlated with each other, or both.

However, it is well known that linear combination of atomic orbital (LCAO) basis sets for correlated calculations have significant linear dependencies in them. The simplest way to attempt to eliminate the linear dependency is to remove several of the highest energy unoccupied (virtual) orbitals from a HF calculation. Except for dropping the core orbitals and the corresponding virtuals, experience has shown that this method is not very successful[25,26]. There have been myriad other attempts at finding a good way to reduce basis set size for correlated calculations throughout the development of quantum chemistry[25,27–29]. Natural orbitals (the eigenfunctions of the single-particle density matrix)[30] are known to be the best way to determine which single particle states are important in the system[30], as recently recognized by the density-matrix renormalization community[31]. Since determining natural orbitals for coupled-cluster theory necessitates solving the full coupled-cluster problem in the full basis, using coupled-cluster natural orbitals is not a possibility[32]. Instead, it has long been known in the CI community that most of their benefit can be gained from using a MBPT(2) density matrix[33–37]. It was proposed[27,28] by one of us to optimize a truncated virtual space by maximizing the MBPT(2) correlation correction using the second-order Hylleraas functional (an upper bound on the second-order energy); this was the so-called optimized virtual orbital space (OVOS) scheme. As an alternative to OVOS, the use of the so-called frozen natural orbitals (FNOs) for virtual space truncation (for example[33,35,38–41]) was investigated, within the coupled-cluster method, for water at equilibrium[26]. Further work showed that for many equilibrium problems, the FNOs are an exceedingly good set of orbitals for truncation[25–28]. Compared to the OVOS procedure, which is based on a purely energetic criterion, the FNO orbitals, derived from the one-particle density matrix, are less tailored to the energy. Because OVOS requires iterative second-order perturbation theory calculations, it is significantly more computationally expensive than the FNO procedure is; the added computational expense yields only a small improvement in the energy[26]. The OVOS method has been recently reinvestigated, with the purely energetic criterion replaced by an overlap criterion[42]; this change may lead to less energy-specific OVOS orbitals, although the computational cost is still high relative to the FNOs.

THEORETICAL METHOD

We determine frozen natural orbitals from a MBPT(2) approximation to the exact density matrix. First, a Hartree–Fock calculation in the full basis set is performed yielding a set of occupied and virtual molecular orbitals (MOs) formed from a linear combination of atomic orbital (AO) basis functions, denoted by the matrix $\boldsymbol{U}$ (where columns are the MOs and rows are AOs). Next, the MBPT(2) single-particle density matrix, $\boldsymbol{D}$, is constructed within only the virtual space of the MO basis. To determine the frozen natural orbitals the eigenvalue equation

$$\boldsymbol{DV} = \boldsymbol{Vn} \tag{1}$$

is solved. The columns of $\boldsymbol{V}$ are the FNOs in the MO basis and the value of the corresponding element of $\boldsymbol{n}$ is the occupation number of that natural orbital. The relative importance of an FNO is given by this occupation number, allowing for truncation of the natural orbitals with occupation less than some cutoff value n_{crit}. Symbolically,

$$\tilde{\boldsymbol{V}} = \boldsymbol{VT} \tag{2}$$

$$T_{ij} = \begin{cases} \delta_{ij} & n_i > n_{\text{crit}} \\ 0 & \text{otherwise} \end{cases} . \tag{3}$$

This reduced set of frozen natural orbitals is then used as a replacement of the full virtual space. To return the orbitals to canonical HF form[43], the virtual–virtual block of the Fock matrix (in the MO basis), $\boldsymbol{F}$, is transformed into the truncated FNO basis and eigenvalue equation for the orbital energies is solved.

$$\tilde{\boldsymbol{F}} = \tilde{\boldsymbol{V}}^{\dagger} \boldsymbol{F} \tilde{\boldsymbol{V}} \tag{4}$$

$$\tilde{\boldsymbol{F}}\tilde{\boldsymbol{Z}} = \tilde{\boldsymbol{Z}}\tilde{\varepsilon} \tag{5}$$

The columns of $\tilde{\boldsymbol{Z}}$ are the new canonical virtual MOs in the FNO basis and the elements of $\tilde{\varepsilon}$ are the corresponding orbital energies. Back-transforming into the AO basis,

$$\tilde{\boldsymbol{U}}_{\text{virt}} = \boldsymbol{U}_{\text{virt}} \tilde{\boldsymbol{V}}\tilde{\boldsymbol{Z}} \tag{6}$$

$$\tilde{\boldsymbol{U}}_{\text{occ}} = \boldsymbol{U}_{\text{occ}} \tag{7}$$

where the subscripts virt and occ indicate the virtual and occupied blocks of the MO matrix, respectively. The matrix $\tilde{\boldsymbol{U}}$ now contains a reduced set of virtual canonical HF orbitals that can be used in a higher-level treatment of correlation; in this case, coupled-cluster theory.

To maintain all the desired symmetry and invariance conditions after the FNO truncation, several conditions were imposed on the truncation matrix. For unrestricted Hartree–Fock (UHF) references, it was required that the number of orbitals removed was the same for both α and β spins. Moreover, the number of orbitals removed within each irreducible representation of the molecular point group was required to be the same. Similarly, for both RHF and UHF references, all degenerate orbitals were treated as a block: either all were kept or all were removed from the FNO basis.

Although there is no requirement that a canonical HF set of orbitals be used, the decoupling of the occupied and virtual spaces in Hartree–Fock is necessary to be able to perform these operations solely on the virtual space. For more general initial orbitals, the same procedure can be applied but the entire set of MOs would be required. In these authors' opinion, for a situation where a single HF determinant provides a good description of the ground state, it is advantageous to leave the occupied space unchanged, and simply truncate the virtual space. Computational scaling of CC is more severe for virtual orbitals than for occupied orbitals implying greater computational advantage truncating the virtual space and the quality of the occupied reference is left unaltered. As experience in CI suggests, for cases with significant multireference character constructing the full set of natural orbitals from a non-HF initial set of orbitals and truncating may be a better choice[33].

Estimates of Truncation Error

The authors have found it useful to estimate the truncation error. An MBPT(2) energy calculation is by default run both for the full basis and after the truncation for the FNO basis. Therefore, we can use the energy difference between these two second-order calculations as an estimate of the error inherent in the truncation. Defining

$$\Delta\text{MBPT(2)} = \text{MBPT(2)[full]} - \text{MBPT(2)[truncated]}. \qquad (8)$$

This correction can then be added to the total energy as calculated in the truncated basis to give a better approximation to the exact energy with no added computational cost.

COMPUTATIONAL DETAILS

The frozen natural orbital truncation scheme has been included into the ACES II quantum chemistry package[44] for RHF and UHF references with real Abelian symmetry. Non-Abelian point group symmetry (though not handled within most ACES II calculations) was enforced by treating all degenerate orbitals as a block. Degeneracy was assumed if two (or more) orbitals had occupations that differed by less than 10^{-6}. Most calculations were performed on an IBM RS/6000 POWER3 workstation with a 375 MHz processor, 3 GB RAM, and 18 GB hard disk. Basis sets used were from the PNL basis set library[45].

Small Molecules

Calculations were run along the symmetric stretch for six small molecules (HF, CO, F_2, H_2O, N_2 and NH_3) at 0.1 Å increments, from a minimum of 0.5 Å to $4R_e$. Results were obtained from both RHF and UHF reference functions, depending on the desired separated limit, with Hartree–Fock stability analysis used to stay on the correct adiabatic potential energy surface during dissociation.

Energetic Materials

For the larger energetic materials, all calculations were done with the frozen core approximation, reducing the number of occupied orbitals. To minimize the amount of time and number of orbitals under investigation, all of these calculations were done with an RHF reference state. For the largest calculations (DMNA in the full cc-pVTZ basis), 18 GB disk space was not sufficient and necessitated the use of a 200 MHz processor with 4 GB RAM and access to storage in excess of 1 TB.

RESULTS AND DISCUSSION

Small Molecules

The quality of frozen natural orbitals for equilibrium properties and for the dipole moment in coupled-cluster theory has been investigated before[25,26]. However, if the FNOs are to be useful for calculating energy differences between different conformers of molecules and along reaction pathways, the quality of the FNOs must be maintained across the potential energy surface, which has also been considered as a special case of OVOS[27]. To gauge this element of the quality, a series of six small molecules were examined across their potential energy surfaces at the CCSD and CCSD(T) level in the DZP[46], cc-pVTZ, and cc-pVQZ[8] bases with retention of 20, 40, 60, 80 and 100% of the virtual orbitals. Average results and timings are listed in Table I.

The best basis set choice for any calculation is the one that can give you the greatest percentage of the correlation energy with the quickest calculation. Figure 1 is a guide for that decision based on the FNO orbital scheme.

The upper-left hand corner of Fig. 1 represents the best possible basis set. As can be seen, choosing a large basis set and then truncating it using the FNO framework provides superior results compared to using a smaller basis

TABLE I
Average percentage of correlation energy for a series of FNO truncations for six small molecules

Virtual orbitals, %	DZP[a]	cc-pVTZ[a]	cc-pVQZ[a]
20	29.6	61.1	81.2
40	47.3	76.0	94.0
60	58.7	82.2	98.0
80	63.1	85.0	99.2
100	66.0	85.6	100

[a] Percentage of correlation energy relative to 100% cc-pVQZ result.

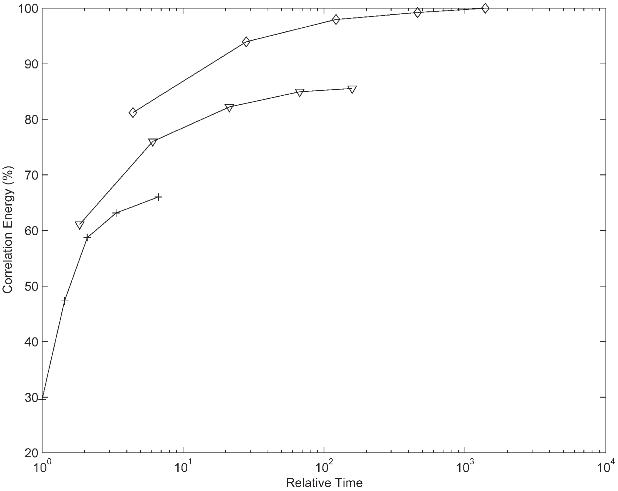

FIG. 1
Percentage of CCSD(T) correlation energy compared to 100% cc-pVQZ result recovered as a function of the coupled-cluster time relative to 20% DZP calculation as a function of basis set. ◇ cc-pVQZ, ▽ cc-pVTZ, + DZP

set. For example, for the molecules considered, using a 40% cc-pVQZ basis set would provide both a greater percentage of the total correlation energy and be a quicker calculation than using the full cc-pVTZ basis set. An illustration of this effect is shown in Fig. 2, which shows four potential energy curves for the dissociation of hydrogen fluoride at the CCSD level in different bases.

The lowest curve is the full 100% cc-pVQZ basis result, the others are truncations from three different bases. The qualitative form of the PES is identical in all four cases, indicating that the FNOs provide a balanced treatment of correlation across the potential energy surface. The best results, after the full cc-pVQZ basis, are those from a retention of 20% of the cc-pVQZ basis. This truncated large basis significantly outperforms the equivalent-sized full DZP basis.

Shifting the energies of these curves so that their equilibria coincide, shows that not only does using an FNO truncated basis lead to convergence with total energies, it also leads to convergence in dissociation energies. Figure 3 shows the dissociative tails of these shifted potential energy surfaces; as can be seen, the 20% cc-pVQZ basis comes closest to accurately describing the dissociation. The full DZP basis underestimates the dissociation energy by more than 20 mE_h, while the 20% cc-pVQZ basis is within 3 mE_h of the full cc-pVQZ dissociation energy.

Energetic Molecules

Two energetic materials were addressed in this study: dimethylnitramine (both the monomer and dimer) and 1,3,5-trinitrohexahydro-1,3,5-triazine.

Dimethylnitramine (DMNA)

The FNO method was used to measure the relative energy of the two DMNA isomers that have been predicted/observed. The calculation was performed in both a DZP and cc-pVTZ basis set, with 60% of the virtual space retained. For comparison and verification, calculations were also done in the full DZP and cc-pVTZ basis sets. The results are summarized in Table II.

The agreement between the full cc-pVTZ and truncated cc-pVTZ energy differences is excellent. Also, note the difference in results at the DZP level between including and not including the ΔMBPT(2) correction. We conjecture that because there are so many fewer virtual orbitals in a DZP basis than in a cc-pVTZ basis a greater percentage of those truncated contain a

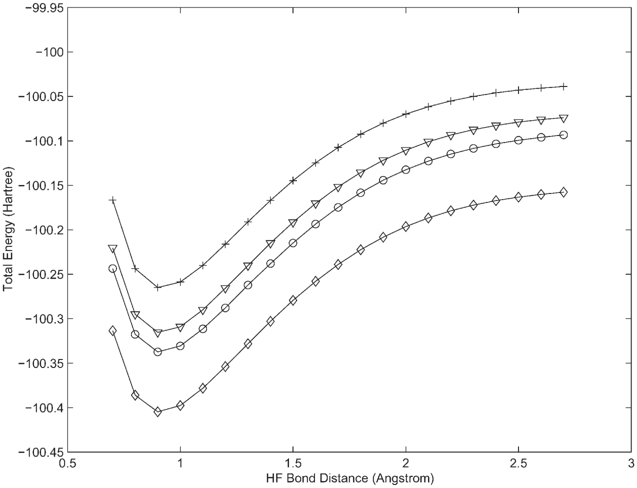

FIG. 2
Hydrogen fluoride RHF CCSD potential energy curve for different FNO basis truncations with the same number of virtual orbitals. ◇ 100% cc-pVQZ, ○ 20% cc-pVQZ, ▽ 40% cc-pVTZ, + 100% DZP

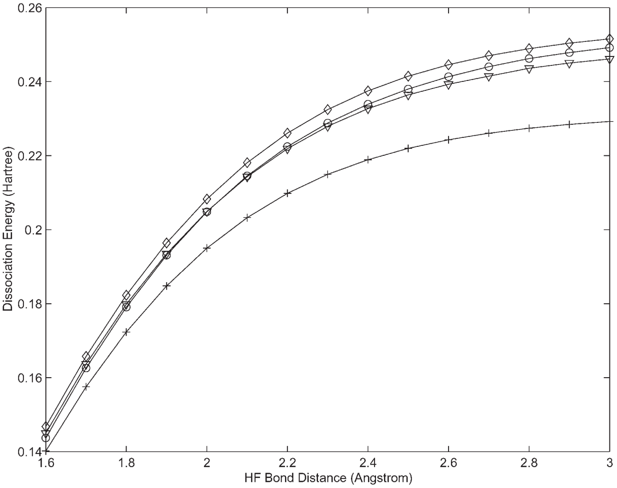

FIG. 3
Hydrogen fluoride RHF CCSD dissociation energy curves for different FNO basis truncations with the same number of virtual orbitals. ◇ 100% cc-pVQZ, ○ 20% cc-pVQZ, ▽ 40% cc-pVTZ, + 100% DZP

significant occupation. Because of this, a correction due to the truncation level is necessary for a small basis set, but not for a larger basis set.

We also applied the FNOs to investigate the dimer of DMNA. Prior work had determined, using symmetry-adapted perturbation theory, five minima structures for rigid geometry C_{2v} monomers[10]. Using their geometries, we calculated interaction energies at the CCSD(T) level of theory, comparison to the SAPT results are shown in Table III.

While the difference in interaction energies between SAPT and CCSD(T) is only on the order of a few kcal/mol, there is a qualitative difference between the two results. The energies of minima M2 and M3 are in the opposite order in the CCSD(T) result compared to the SAPT results. Determining the correct energetic ordering will require validation of the FNO method for

TABLE II

DMNA RHF CCSD(T) frozen core energy differences

Basis set used	C_{2v} E_{tot}[a]	C_s E_{tot}[a]	$C_{2v} - C_s$ kcal/mol	Total time, h
100% DZP	–338.8157	–338.8302	9.09	1.61
60% DZP	–338.7549	–338.7671	7.66	0.25
60% DZP + ΔMBPT(2)	–338.8078	–338.8220	8.91	0.25
100% cc-pVTZ	–339.1252	–339.1399	9.24	52.6[b]
60% cc-pVTZ	–339.1032	–339.1180	9.29	8.80
60% cc-pVTZ + ΔMBPT(2)	–339.1283	–339.1431	9.29	8.80

[a] Total energies are in E_h. [b] Approximate time taking into account the difference in processor speed.

TABLE III

DMNA dimer RHF CCSD(T) interaction energies at SAPT geometries

SAPT Minimum[b]	SAPT Interaction energy[c]	CCSD(T)[a] Interaction energy[c]
M1	–11.056	–10.355
M2	–5.934	–3.821
M3	–5.169	–5.602
M4	–4.855	–2.379

[a] 60% DZP basis + ΔMBPT(2). [b] For geometries, see ref.[10] [c] Interaction energies in kcal/mol.

interaction energies, full geometry optimization of the dimers at the FNO level, larger basis sets, consideration of basis set superposition error; and may require inclusion of iterative triple excitations.

1,3,5-Trinitrohexahydro-1,3,5-triazine (RDX)

Chakraborty et al.[13] gave two minima structures for RDX: the AAA chair and the AAA boat. They performed B3LYP calculations on these minima, and found that at that level of theory, the AAA chair was 0.75 kcal/mol lower in energy than the AAA boat. They also found (by performing a vibrational analysis) that the AAA boat was not a minimum for B3LYP. We used their geometries for both conformers and performed a frozen core RHF CCSD(T) calculation in a 60% DZP FNO basis. Table IV lists the results.

The energy difference at these two geometries determined by 60% DZP CCSD(T) is –1.4 kcal/mol, on the same order as the B3LYP result –0.75 kcal/mol. Further calculations in a (truncated) triple zeta basis and with full geometry optimization are necessary to definitively determine which conformation is lower in energy.

CONCLUSIONS

On the basis of the results presented here it is clear that frozen natural orbitals determined from the MBPT(2) density matrix are an effective method of basis set truncation. The quality of the basis set truncation does not appear to degrade at large R as might be expected given that MBPT(2) is a perturbative method. However, we can equally well use UHF MBPT(2) in our FNO generation if bond dissociation becomes a problem. More detailed

TABLE IV
RDX RHF CCSD(T) 60% DZP frozen core energy difference

Calculation	AAA chair[a]	AAA boat[a]	Chair–boat
Total energy[b]	–895.1732	–895.1728	–0.25
Total energy + ΔMBPT(2)[b]	–895.3311	–895.3289	–1.4
Time, h[c]	30	145	N/A
Estimated time for full basis, h[c]	200	1000	N/A

[a] Geometries from ref.[13] [b] Total energies in E_h, relative energies in kcal/mol. [c] For coupled-cluster calculation.

analysis has shown that differences between the FNO correlation and the full correlation energy is roughly constant across the PES [27,28]. Because the total correlation energy is smaller at large R than short R, the percentage of correlation energy recovered in a truncated calculation increases with increasing R. This percentage increase is small in general (and the smaller the larger the basis set used) and had no impact on the qualitative features of the PES in our calculations. As was shown for the case of HF, this slight increase in correlation energy across the PES does not adversely affect the description of dissociative processes.

The FNOs are a powerful tool toward allowing coupled-cluster theory to address larger molecules routinely. Most importantly, unlike many linear scaling or truncation methods, the FNOs require no user analysis of the molecule to determine what regions of the molecule should be correlated. Instead, the important interactions are determined by the method itself, without any input of chemical intuition. Further, the tools necessary to determine and truncate based on the FNOs are already built into coupled-cluster programs, making it straight-forward to implement.

Current limitations in the ACES II program allow only a maximum of 500 basis functions, restricting the calculation of the FNOs to systems with fewer orbitals than that. As our results show, if we were able to calculate the MBPT(2) density matrix with greater than 500 basis functions, truncation by the FNOs could significantly reduce the number of basis functions for the coupled-cluster iterations. Therefore, the actual calculation of the MBPT(2) density matrix is the limiting step in the current implementation. We plan on interfacing an integral-direct MBPT(2) program that will circumvent the 500 basis function limit.

To be routinely applicable to all chemical situations, analytical gradients must be used so that geometry optimization and forces are available. The equations for FNO analytical gradients have been derived and have been implemented and tested in the ACES II code[47].

This work has been supported the U.S. Army Research Office under MURI (Contract No. AA-5-72732-B1). A. G. Taube would also like to thank the U.S. Air Force Office of Scientific Research for support through a National Defense Science and Engineering Graduate Fellowship.

REFERENCES

1. Stolevik R., Rademacher P.: *Acta Phys. Scand.* **1969**, *23*, 672.
2. Krebs B., Mandt J.: *Acta Crystallogr. B: Struct. Crystallogr. Cryst. Chem.* **1979**, *35*, 402.
3. Khaikin L., Grikina O., Vilkov L., Palafox M., Boggs J.: *J. Struct. Chem.* **1993**, *34*, 2.

4. Smith G. D., Bharadwaj R. K., Bedrov D., Ayyagari C.: *J. Phys. Chem. B* **1999**, *103*, 705.
5. Johnson M. A., Truong T. N.: *J. Phys. Chem. A* **1999**, *103*, 8840.
6. Harris N. J., Lammertsma K.: *J. Phys. Chem. A* **1997**, *101*, 1370.
7. Hariharan P., Pople J.: *Theor. Chim. Acta* **1973**, *28*, 213.
8. Dunning T., Jr.: *J. Chem. Phys.* **1989**, *90*, 1007.
9. Adams G. F., Robert J., Shaw W.: *Annu. Rev. Phys. Chem.* **1992**, *43*, 311.
10. Bukowski R., Szalewicz K., Chabalowski C. F.: *J. Phys. Chem. A* **1999** *103*, 7322.
11. Rice B. M., Chabalowski C. F.: *J. Phys. Chem. A* **1997**, *101*, 8720.
12. Harris N. J., Lammertsma K.: *J. Am. Chem. Soc.* **1997**, *119*, 6583.
13. Chakraborty D., Muller R. P., Dasgupta S., Goddard W. A., III: *J. Phys. Chem. A* **2000**, *104*, 2261.
14. Raghavachari K., Trucks G., Pople J., Head-Gordon M.: *Chem. Phys. Lett.* **1989**, *157*, 479.
15. Purvis G. D., Bartlett R. J.: *J. Chem. Phys.* **1982**, *76*, 1910.
16. Watts J. D., Gauss J., Bartlett R. J.: *J. Chem. Phys.* **1993**, *98*, 8718.
17. Hampel C., Werner H.-J.: *J. Chem. Phys.* **1996**, *104*, 6286.
18. Flocke N., Bartlett R. J.: *J. Chem. Phys.* **2004**, *121*, 10935.
19. Koch H., Sáchez de Merás A., Pederson T. B.: *J. Chem. Phys.* **2003**, *118*, 9481.
20. Kinoshita T., Hino O., Bartlett R. J.: *J. Chem. Phys.* **2003**, *119*, 7756.
21. Hino O., Kinoshita T., Bartlett R. J.: *J. Chem. Phys.* **2004**, *121*, 1206.
22. Klopper W., Kutzelnigg W.: *Chem. Phys. Lett.* **1987**, *134*, 17.
23. Kutzelnigg W., Klopper W.: *J. Chem. Phys.* **1991**, *94*, 1985.
24. Klopper W., Kutzelnigg W.: *J. Chem. Phys.* **1991**, *94*, 2020.
25. Wilson K. J.: *Ph.D. Thesis*. University of Florida, Gainesville (FL) 2002.
26. Sosa C., Geertsen J., Trucks G. W., Bartlett R. J., Franz J. A.: *Chem. Phys. Lett.* **1989**, *159*, 148.
27. Adamowicz L., Bartlett R. J.: *J. Chem. Phys.* **1987**, *86*, 6314.
28. Adamowicz L., Bartlett R. J., Sadlej A. J.: *J. Chem. Phys.* **1988**, *88*, 5749.
29. Mintz B., Lennox K. P., Wilson A. K.: *J. Chem. Phys.* **2004**, *121*, 5629.
30. Löwdin P.-O.: *Phys. Rev.* **1955**, *97*, 1474.
31. White S. R.: *Phys. Rep.* **1998**, *301*, 187.
32. In terms of truncation techniques. For an example of the use of CC NOs in other methods see: Abrams M. L., Sherill C. D.: *Chem. Phys. Lett.* **2004**, *395*, 227.
33 Jørgen H., Jensen A., Jørgensen P., Ågren H., Olsen J.: *J. Chem. Phys.* **1988**, *88*, 3834.
34. Meyer W. in: *Methods of Electronic Structure* (H. F. Schaefer, III, Ed.), p. 413. Plenum Press, New York 1977.
35. Barr T. L., Davidson E. R.: *Phys. Rev. A* **1970**, *1*, 644.
36. Meyer W.: *J. Chem. Phys.* **1973**, *58*, 1017.
37. Hay P. J.: *J. Chem. Phys.* **1973**, *59*, 2468.
38. Ahlrichs R., Lischka H., Staemmler V., Kutzelnigg W.: *J. Chem. Phys.* **1975**, *62*, 1225.
39. Edmiston C., Krauss M.: *J. Chem. Phys.* **1966**, *45*, 1833.
40. Ahlrichs R., Kutzelnigg W.: *Theor. Chim. Acta* **1968**, *10*, 377.
41. Gelus M., Ahlrichs R., Staemmler V., Kutzelnigg W.: *Chem. Phys. Lett.* **1970**, *7*, 503.
42. Neogrády P., Pitoňák M., Urban M.: *Mol. Phys.*, in press.
43. We just as easily can leave the orbitals as is due to the invariance of coupled-cluster theory to unitary rotations within, separately, the occupied and virtual space. However, the Fock matrix must be recalculated in either case and without the back-rotation one loses the simplicity of canonical HF.

44. *ACES II* is a program product of the Quantum Theory Project, University of Florida, Gainesville (FL) 1990. Authors: Stanton J. F., Gauss J., Perera S. A., Yau A., Watts J. D., Nooijen M., Oliphant N., Szalay P. G., Lauderdale W. J., Gwaltney S. R., Beck S., Balková A., Bernholdt D. E., Baeck K. K., Rozyczko P., Sekino H., Huber C., Pittner J., Bartlett R. J.. Integral packages included are *VMOL* (Almlöf J., Taylor P. R.); *VPROPS* (Taylor P.); *ABACUS* (Helgaker T., Jensen H. J. Aa., Jørgensen P., Olsen J., Taylor P. R.).
45. Basis sets were obtained from the *Extensible Computational Chemistry Environment Basis Set Database*, Version 1.0, as developed and distributed by the Molecular Science Computing Facility, Environmental and Molecular Sciences Laboratory which is part of the Pacific Northwest Laboratory, P.O. Box 999, Richland, WA 99352, U.S.A., and funded by the U.S. Department of Energy. The Pacific Northwest Laboratory is a multi-program laboratory operated by Battelle Memorial Institute for the U.S. Department of Energy under contract DE-AC06-76RLO 1830. Contact David Feller, Karen Schuchardt, or Don Jones for further information.
46. Dunning T., Jr.: *J. Am. Chem. Soc.* **1979**, *101*, 2856.
47. Taube A. G., Bartlett R. J.: Unpublished results.